Pediatric Cardiology
https://doi.org/10.1007/s00246-017-1785-4

ORIGINAL ARTICLE

Comparison of 3D Echocardiogram-Derived 3D Printed Valve Models to Molded Models for Simulated Repair of Pediatric Atrioventricular Valves

Adam B. Scanlan[1] · Alex V. Nguyen[1] · Anna Ilina[2] · Andras Lasso[2] · Linnea Cripe[1] · Anusha Jegatheeswaran[4] · Elizabeth Silvestro[3] · Francis X. McGowan[1] · Christopher E. Mascio[5] · Stephanie Fuller[5] · Thomas L. Spray[5] · Meryl S. Cohen[4] · Gabor Fichtinger[2] · Matthew A. Jolley[1,4]

Received: 7 September 2017 / Accepted: 22 November 2017

Abstract

Mastering the technical skills required to perform pediatric cardiac valve surgery is challenging in part due to limited opportunity for practice. Transformation of 3D echocardiographic (echo) images of congenitally abnormal heart valves to realistic physical models could allow patient-specific simulation of surgical valve repair. We compared materials, processes, and costs for 3D printing and molding of patient-specific models for visualization and surgical simulation of congenitally abnormal heart valves. Pediatric atrioventricular valves (mitral, tricuspid, and common atrioventricular valve) were modeled from transthoracic 3D echo images using semi-automated methods implemented as custom modules in 3D Slicer. Valve models were then both 3D printed in soft materials and molded in silicone using 3D printed "negative" molds. Using pre-defined assessment criteria, valve models were evaluated by congenital cardiac surgeons to determine suitability for simulation. Surgeon assessment indicated that the molded valves had superior material properties for the purposes of simulation compared to directly printed valves ($p < 0.01$). Patient-specific, 3D echo-derived molded valves are a step toward realistic simulation of complex valve repairs but require more time and labor to create than directly printed models. Patient-specific simulation of valve repair in children using such models may be useful for surgical training and simulation of complex congenital cases.

Keywords 3D printing · Surgical simulation · Valve repair · 3D echocardiography

Abbreviations

3D	Three-dimensional
2D	Two-dimensional
3DE	Three-dimensional echocardiogram
Echo	Echocardiogram
DICOM	Digital imaging in medicine
CAVC	Complete atrioventricular canal
HLHS	Hypoplastic left heart syndrome

Adam B. Scanlan and Alex V. Nguyen contributed equally to this work.

✉ Matthew A. Jolley
JOLLEYM@email.chop.edu

[1] Department of Anesthesiology and Critical Care Medicine, Children's Hospital of Philadelphia, 3401 Civic Center Blvd, Philadelphia, PA 19104, USA

[2] Laboratory for Percutaneous Surgery, Queen's University, Kingston, ON, USA

[3] Department of Radiology, Children's Hospital of Philadelphia, Philadelphia, PA, USA

[4] Division of Pediatric Cardiology, Children's Hospital of Philadelphia, Philadelphia, PA, USA

[5] Division of Cardiothoracic Surgery, Children's Hospital of Philadelphia, Philadelphia, PA, USA

Introduction

Atrioventricular valves are complex three-dimensional (3D) structures. The development and successful utilization of valve repair techniques has been predicated on understanding the valve mechanics underlying dysfunction. This began with physical inspection of the valve in the flaccid heart by Carpentier [1–3]. The development of 2D and then 3D echocardiograms (3DE) gave surgeons the means to examine the beating heart, and the echocardiographer has become an essential part of both surgical planning and postoperative assessment of repair [4, 5].

Published online: 27 November 2017

Successful valve repair in pediatrics has long been a goal due to the hazards and complications of prosthetic valves and serial valve replacement in very small and growing children [6]. In the modern era, efforts to improve valve repair in children continue with various techniques borrowed from adult valve repair [7]. Valve repair is also an integral component of complex congenital heart surgeries for the repair of complete atrioventricular canal (CAVC). While technology has allowed for 3D volume rendered images on a flat screen, these images are limiting in terms of translation of visual information into surgical understanding of valve structure. And while surgical simulation has been shown to be of benefit in a broad range of surgical disciplines, including cardiac surgery, translation of 3DE to patient-specific valve models suitable for simulation has not occurred [8–12]. Thus, the need exists for valve model-based simulation training in pediatric and congenital cardiac valve repair, as many anomalies are rare and heterogeneous, and there is an expectation that the senior surgeon, rather than trainee, performs these complex repairs.

The advent of 3D printed valves based on 3DE data in rigid material has allowed physical creation of patient-specific mitral and aortic valve models from 3DE data [13–15]. However, barriers to simulated valve repair in children remain. First, pediatric modeling requires modeling software that accommodates multiple congenitally abnormal valve types (mitral, tricuspid, CAVC). Currently there is no commercial platform dedicated to this purpose, and patient-specific 3D physical models of pediatric or congenitally abnormal heart valves for simulated valve repair are not available. Second, to realistically simulate valve repair, "valve-like" materials must be pliable and elastic enough to be cut and sewn.

In this study, we sought to improve upon previous physical 3D valve modeling and extend modeling to pediatric and congenital heart disease using transthoracic 3DE images [13–17]. We describe novel software that we developed to create high-fidelity, patient-specific pediatric atrioventricular valve models from transthoracic 3DE images. Models were created by (1) 3D printing valve models in soft materials and (2) creating molded silicone valve models from 3D printed molds. We hypothesized that molded silicone valves would have superior material properties for surgical simulation compared to best currently available directly printed materials.

Materials and Methods

Subjects

An institutional database was used to retrospectively identify patients with high-quality 3DE performed for clinical indications. Echocardiograms from a 15-year-old female with hypoplastic left heart syndrome (HLHS), a 4-day-old male with HLHS, a 15-year-old male with a normal mitral valve, a 3-month-old female with CAVC, and a 1-day-old male with CAVC were utilized in this study. The study was approved by the Institutional Review Board at The Children's Hospital of Philadelphia.

Transthoracic Image Acquisition and 2D Echo Data

3DE of atrioventricular valves were routinely acquired as part of clinical protocols, acquired using Full Volume or 3D Zoom mode, with 4–6 beat breath-held ECG-gated acquisitions when possible. Transthoracic X7 or X5 probes were used with the Philips IE33 and EPIQ ultrasound systems (Philips Medical, Andover, MA).

3D Mitral Valve Model Creation and Direct 3D Printing

Valve modeling was done in custom software created in the 3D Slicer [18]. 3DE images were anonymized, exported to Digital Imaging Communication in Medicine (DICOM) format, converted to Cartesian DICOM in QLab (Philips Medical, Andover, MA), and imported into the custom SlicerHeart software. A single mid-systolic frame was chosen for static modeling and analysis of the valve.

The annular curve was traced by rotating image cutting planes around the annulus in 10-degree increments, generating 36 points which were then smoothed using Fourier smoothing and resampled to a smooth curve to define the annular boundary (Fig. 1). Individual valve leaflets were segmented using thresholding and manual touchup followed by smoothing with a median filter (Figs. 1 and 2).

Because the thickness derived from 3D ultrasound appeared to result in unrealistically thick valves (iterative surgical feedback), we extracted the atrial surface of the valve to create a manifold surface from which arbitrarily thick leaflets could be specified based on surgical input and pathology review (Fig. 3). Once models were finalized, a boundary ring for mounting into a simulation holder was added (Fig. 3). The final valve within the mounting ring was then directly 3D printed on an Objet 500 Connex printer (Stratasys, LTD, Eden Prairie, MN) in TangoPlus FLX 930 (Stratasys, LTD, Eden Prairie, MN), the softest, most flexible material (Shore A hardness of 26–28) available for our printer.

Valve Mold Creation and Valve Fabrication

The above models were utilized as the template to create two-piece valve molds in 3D Slicer (Fig. 3). These molds were printed in hard plastic (VeroGray RDG850,

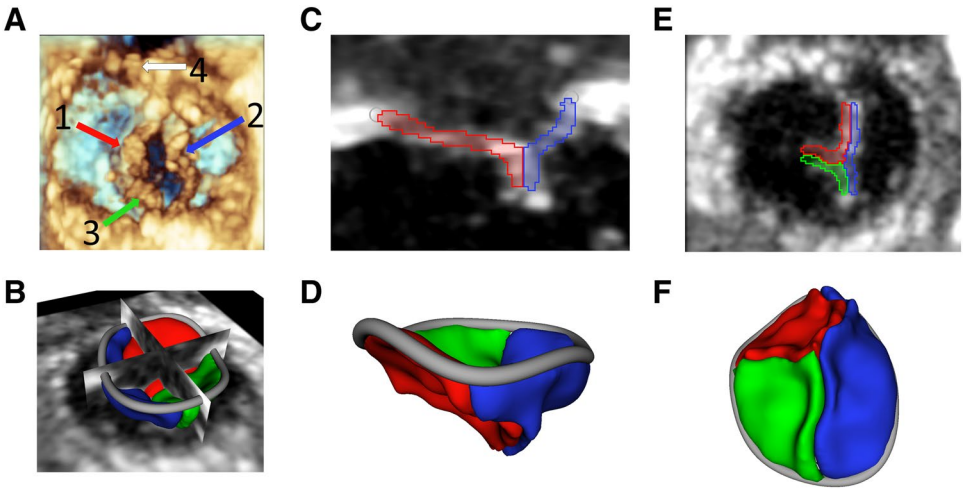

Fig. 1 Tricuspid valve in 4-day-old infant with HLHS: **a** 3D echo view of the ventricular face of the tricuspid valve with the (*1*) anterior leaflet, (*2*) septal leaflet, (*3*) posterior leaflet, and (*4*) native pulmonary valve visible; **b** 3D segmentation of the tricuspid valve displayed with 2D planes; **c** 2D plane showing anterior and septal leaflets; **d** 3D segmentation of the valve from anterior view; **e** 2D plane of coaptation as seen from the ventricle; **f** 3D segmentation as seen from the ventricle

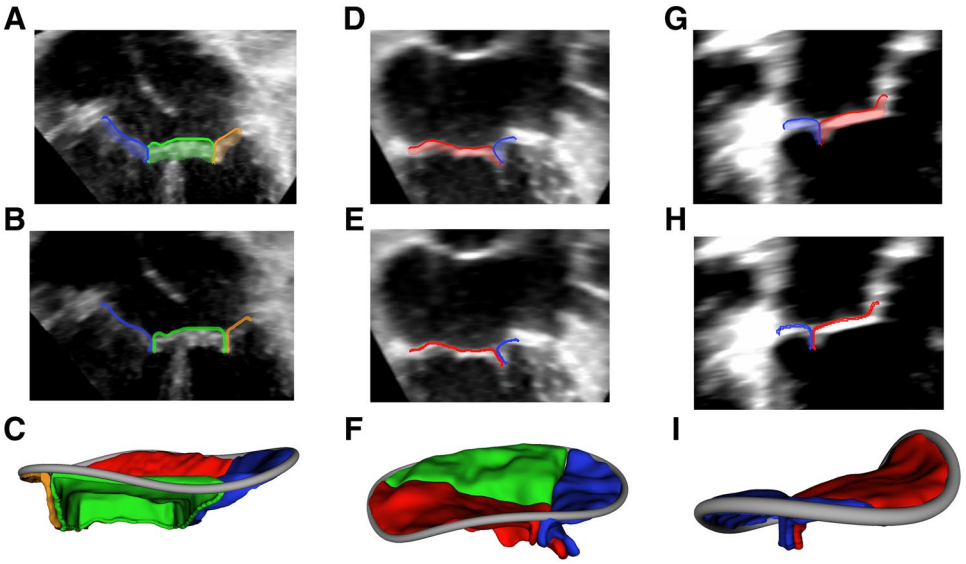

Fig. 2 Examples of valve segmentations and atrial surface extraction: **a** 2D view of segmented CAVC; **b** atrial surface extraction of CAVC; **c** 3D rendering of thickened atrial surface of CAVC for modeling; **d** 2D view of segmented tricuspid; **e** atrial surface extraction of tricuspid; **f** 3D rendering of thickened atrial surface of tricuspid for modeling; **g** 2D view of segmented mitral; **h** atrial surface extraction of mitral; **i** 3D rendering of thickened atrial surface of mitral for modeling

or VeroBlue GDG840, Stratasys, LTD, Eden Prairie, MN) on the Objet 500 printer. Molds were sprayed with Ease Release (Smooth-On, Macungie, PA) (Figs. 4 and 5). Dragon Skin Fast or Medium silicone parts A and B (Smooth-On, Macungie, PA) were combined with Slacker (Smooth-On, Macungie, PA), and then the silicone was degassed in a 5 L degassing chamber (Arksen, City of Industry, CA) and connected to a vacuum pump at − 27 in Hg (GAST Manufacturing, Benton Harbor, MI) for 1.5 min. The silicone was applied to the mold pieces before placing back in the degassing chamber. Models were then set aside to cure, resulting in a valve model (Fig. 3f).

Comparison of 3D Models to Image-Based Measurements

The antero-posterior and lateral dimensions of each valve were measured virtually in QLab (Philips Medical, Andover, MA) and 3D Slicer. The printed models and molded models were directly measured with a digital caliper (Fig. 6).

Surgical Simulation and Comparison of Directly Printed to Molded Valves

Valve models were mounted in a valve holder (LifeLike BioTissue, London, ON). Directly printed valves and molded

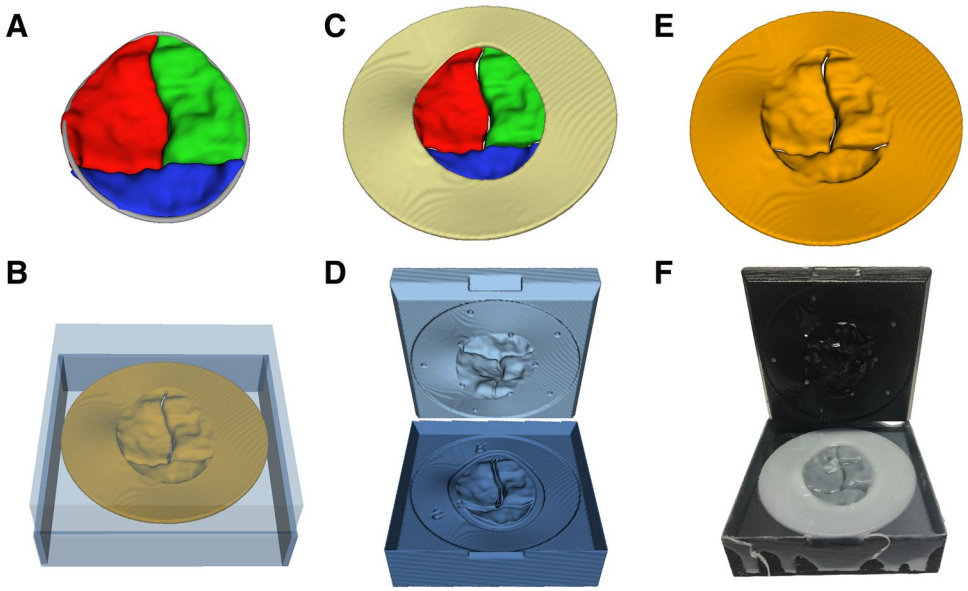

Fig. 3 Creation of 3D printed valve molds: **a** valve segmentation; **b** valve segmentation with addition of valve skirt; **c** model ready for direct printing; **d** automatically generated mold around direct printing template; **e** rendering of upper and lower mold pieces; **f** molded valve in mold

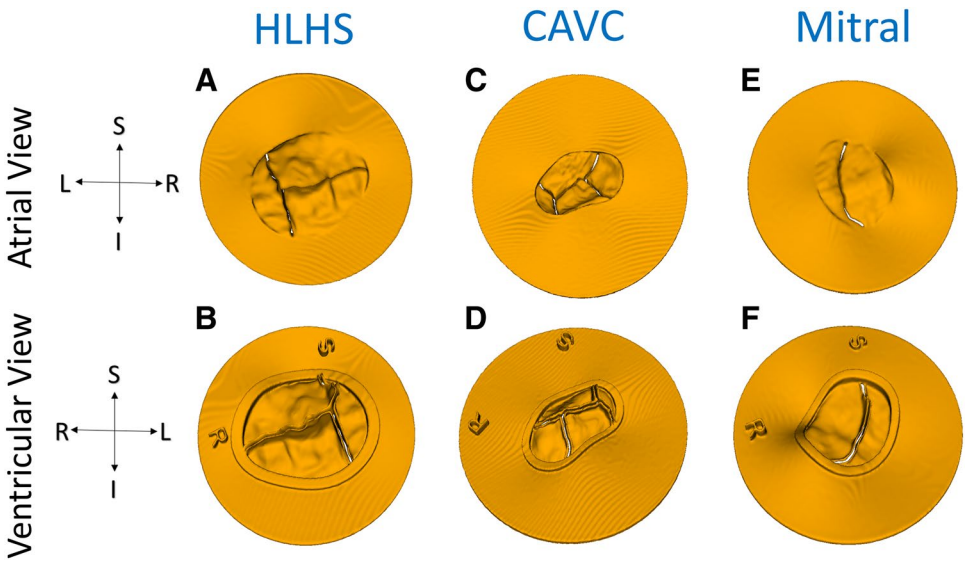

Fig. 4 Models ready for direct 3D printing from atrial and ventricular viewpoints: **a** and **b** tricuspid in HLHS; **c** and **d** CAVC; **e** and **f** mitral. Note preservation of coaptation with a small gap artificially created to ensure the ability to separate leaflets after printing. The coaptation gap for the tricuspid and mitral was 0.3 and 0.2 mm for the mitral

valves for a tricuspid valve in a patient with HLHS and a CAVC were presented to 4 attending physicians and 4 pediatric cardiac surgery fellows. Participants were asked to perform a tricuspid valve annuloplasty and the ventricular component of an atrioventricular canal repair (Figs. 7 and 8). A survey comparison was then given to the surgeon to assess the overall simulation quality as well as compare directly printed to molded valves using defined criteria (Table 3).

Statistical Analysis

Comparison of printed valves to molded valves was done using the Wilcoxon Signed-rank test. Comparison of fellow responses to attending responses was done with the Wilcoxon Rank-Sum Test. These and other descriptive statistics were prepared in IBM SPSS version 21.0 (IBM corporation, Armonk, NY, USA).

Results

Three representative images were selected for simulation, including a mitral valve, CAVC, and tricuspid valve in HLHS. Times and materials cost for virtual model creation and fabrication are shown in Table 1.

Software was developed within 3D Slicer, a free and open-source program for medical image visualization and analysis. The 3D printer utilized was freely available for

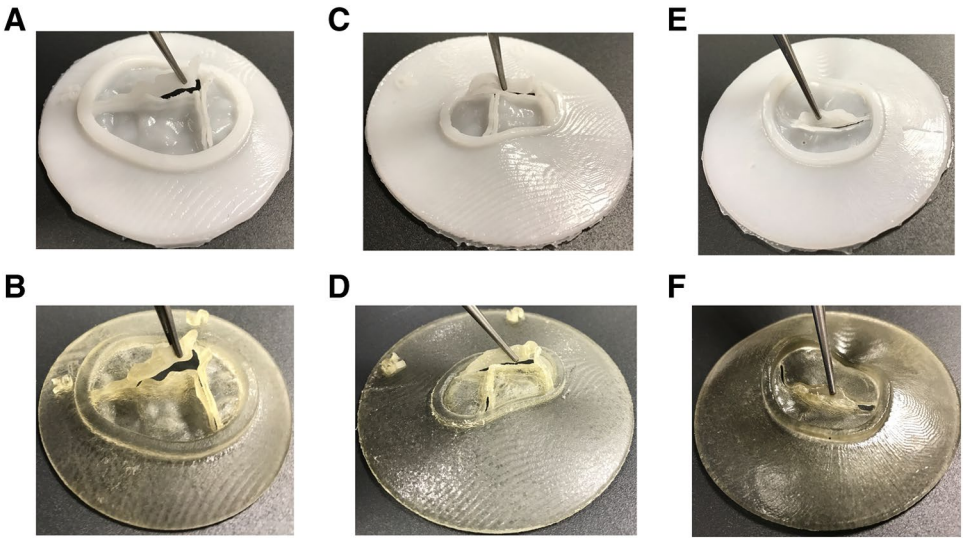

Fig. 5 Molded and printed valve models: **a** molded tricuspid valve; **b** printed tricuspid valve; **c** molded CAVC valve; **d** printed CAVC valve; **e** molded mitral valve; **f** printed mitral valve. Note preservation of coaptation surfaces

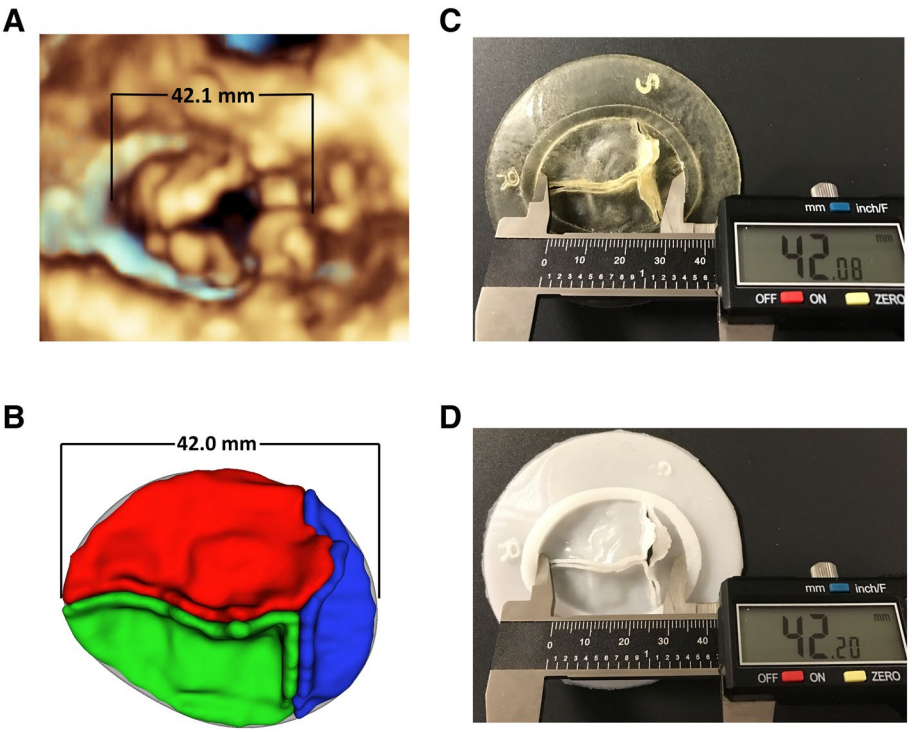

Fig. 6 Comparison of measurements: **a** tricuspid valve rendered in QLab; **b** valve segmentation in 3D Slicer; **c** directly printed valve measured with calipers; **d** molded valve measured with calipers

academic use at the Children's Hospital of Philadelphia, with an original purchase cost of approximately $250,000 in 2011.

The physical size of the valve models were reproduced with high fidelity compared to measurements of echo images in Philips QLab and 3D Slicer (Table 2). Results of surgical evaluation are shown in Table 3. The molded valves were significantly more realistic for cutting and suturing ($p < 0.01$). Successful tightening of annuloplasty suture was highly rated with the molded valves but not the directly printed valves ($p < 0.001$). CAVC repair was highly rated by surgical staff using the molded valves compared to the directly printed valves ($p < 0.01$). Ratings of utility of valve models for training and simulation of difficult cases between attending and fellows were not significantly different ($p > 0.10$).

Discussion

While basic 3D printing offers an opportunity for "passive" evaluation (i.e., patients' or students' education), simulation of surgical interventions requires a more advanced,

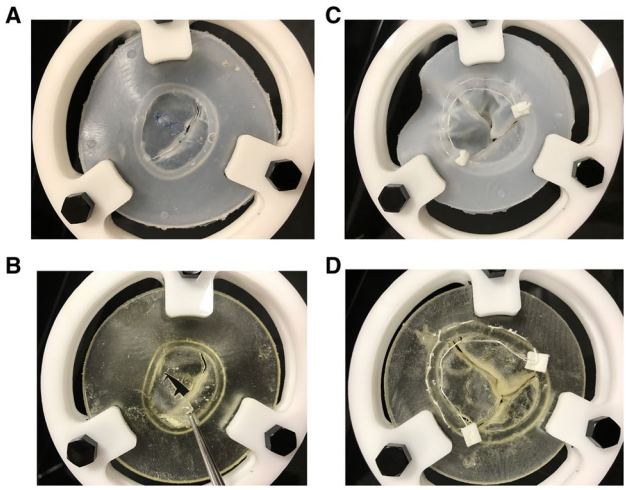

Fig. 7 Simulated valve surgery in molded (top) and directly printed valves(bottom) **a** molded silicone valve cuts and realistically holds suture; **b** directly printed valve is relatively brittle when cutting and tears easily at suture sites; **c** simulated annuloplasty on tricuspid molded valve demonstrating realistic "cinching" of the suture to reduce the annular circumference; **d** simulated annuloplasty on directly printed valve does not cinch and excessive suture tension results in tearing through relatively brittle material

time-consuming, and costly methodology to obtain realistic models. We present a description of the feasibility and accuracy of 3DE-derived 3D printed models of pediatric atrioventricular valves and demonstrate the relative superiority of molded silicone valves to directly printed models for valve repair simulation using current technology. Although not optimized for clinical use, this work describes a necessary step towards the development of cardiovascular 3D printing for pediatric valve surgery simulation and heart surgeon training. This is also the first description of an evolving, pediatric-focused valve modeling toolkit based on open-source software.

Image Quality

Model creation is entirely dependent on 3DE datasets. In general, if leaflets are clearly visible in the image, models can easily be created. ECG-gated, multi-beat studies, enabled by breath holds, improve the temporal and spatial resolution of 3D studies but rely on timing between breaths and are challenging in younger children.

To obtain high-quality images, we developed two pathways for acquisition at our institution: (1) as part of clinical workflows and (2) dedicated breath-held acquisitions while under general anesthesia for clinical indications. When children are younger, dedicated, breath-held 4–6 beat gated acquisitions can reliably provide excellent images (Fig. 1a). Improvements in ultrasound technology may attenuate the benefits of gating and allow high frame rate, high-resolution studies in single-beat acquisitions [19–21]. Further development of miniaturized transesophageal 3D probes will provide an alternative source of high-quality data and increase opportunities for modeling in smaller children in the perioperative setting [22].

Development of Novel Computer Software

While recent publications have summarized the applicability of 3D printing to the adult population, we developed tools specifically for modeling the pediatric and congenital population in concert with the development of fabrication techniques to make resulting physical valve models suitable

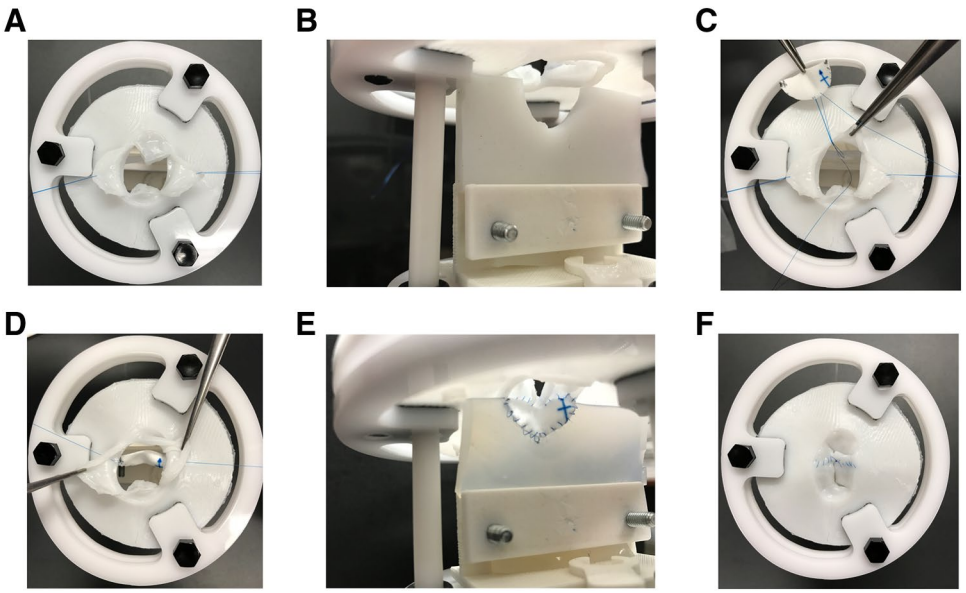

Fig. 8 Simulated repair of CAVC with ventricular 3D printed ventricular septal holder (**b** and **e**); **a** bridging leaflets are pulled back; **b** view of ventricular septal defect prior to insertion of patch; **c** and **d** suturing of patch to VSD; **e** and **f** final view of completed CAVC simulation from the atrial perspective (**e**) and ventricular perspective (**f**)

Table 1 Comparison of model creation pathways

Variable	Mitral		Tricuspid		CAVC	
	DP	Molded	DP	Molded	DP	Molded
Time to create virtual model (h)	0.7	0.7	2.7	2.7	6.2	6.2
Physical model creation						
Time to 3D print (h)	1.6	3.7	1.6	3.7	1.6	3.7
Fast silicone working time (h)	NA	0.13	NA	0.13	NA	0.13
Fast silicone curing time (h)	NA	1.5	NA	1.5	NA	1.5
Medium silicone working time (h)	NA	0.33	NA	0.33	NA	0.33
Medium silicone curing time (h)	NA	5.0	NA	5.0	NA	5.0
Total model creation time (h)	2.3	6.0/9.7[a]	4.3	8.0/11.7[a]	7.8	11.5/15.2[a]
Materials costs						
Print costs (USD)	7.90	43.51	7.90	43.51	7.90	43.51
Silicone cost (USD)	NA	1.49	NA	1.49	1.08[b]	2.57
Cost per 10 valves (USD)	79.00	58.41	79.00	58.41	89.80	69.21

DP (directly printed), Fast silicone (Dragon Skin® Fast), Medium silicone (Dragon Skin® Medium)

[a]Fast silicone/medium silicon

[b]Cost of silicone for septum model

Table 2 Measurement fidelity

Variable	QLab	3D Slicer	Directly printed	Molded
CAVC				
Antero-posterior diameter (mm)	18.1	18.0	18.2	18.1
Septal-lateral diameter (mm)	31.8	31.8	31.7	31.6
Tricuspid (HLHS)				
Antero-posterior diameter (mm)	34.7	34.6	34.8	34.7
Septal-lateral diameter (mm)	42.1	42.0	42.1	42.2
Mitral				
Antero-posterior diameter (mm)	27.3	27.1	27.3	27.2
Septal-lateral diameter (mm)	29.8	29.8	30.0	29.9

CAVC complete atrioventricular canal, *HLHS* hypoplastic left heart syndrome

Table 3 Comparison of surgical evaluation of directly printed and molded valves on 1–5 scale

Variable	Directly printed	Molded	*p* value
Visually realistic	3.5 [1.0–4.0]	4.0 [4.0–4.75]	0.04
Leaflet thickness	2.0 [1.0–4.0]	4.0 [1.5– 4.75]	0.11
Leaflet flexibility	1.5 [1.0–2.0]	4.0 [3.0–4.0]	0.02
Annular rigidity	1.5 [1.0–2.0]	4.0 [2.5–4.75]	0.02
Suturing	1.0 [1.0–1.0]	4.0 [3.25–4.0]	0.01
Annuloplasty simulation	1.0 [1.0–1.0]	4.0 [3.0–4.0]	0.02
CAVC repair simulation	1.0 [1.0–2.75]	4.0 [3.25–4.0]	0.03

Values listed are median [IQR]

p values for Wilcoxon signed-rank test

1–5 scale: 1 (very unrealistic)–5 (very realistic)

for simulation [13–15]. Unlike adults where mitral valve repair represents a large, relatively homogeneous population, pediatric tools will need to be adapted to relatively small, heterogeneous, but equally important populations. This study presents the use of an evolving pediatric-focused toolkit based on the free and open-source 3D Slicer platform. While proprietary segmentation software also allows import of 3D echocardiographic data, these packages are expensive, limiting availability, and utilization. Most importantly, open-source applications can be customized and iteratively improved by the end user. For example, we are actively working on using shape analysis to extract the annular and leaflet contours, facilitating not only visualization, but quantification of 3D valve pediatric valve structure in tricuspid, and CAVC valves for which proprietary analysis tools are not currently available [23].

We have released the converter utilized in this project to convert QLab Philips Cartesian DICOM to a readable format in the SlicerHeart extension for 3D Slicer, but the converter requires access to QLab and the converted images may not maintain full resolution available to native format. This highlights the lack of a standard, open, and consistent

format for 3DE volumetric data. The desire to protect proprietary advances is understandable, but providing conversion to a standard, lossless 3D echo file format would allow unencumbered access to data and fuel advancement of the field particularly in pediatrics where the relatively low volume and heterogeneous population is unlikely to be the focus of commercially developed applications.

Our methodology uses image-processing techniques to capture the full thickness and volume of the valve as represented in the ultrasound image, as opposed to more basic, point-based techniques [24]. Utilizing the full information available in the echo image of the valve also allows the incorporation of semi-automatic or fully automatic segmentation-based image-processing techniques [25, 26]. However, our experience in serial evaluation with surgeons and pathologic specimens suggested that the thickness represented by 3DE was greater than that expected clinically and pathologically, and the thickness of the valves resulting from direct segmentation of the images may be overestimated depending on gain and artifact. As such, we extracted the atrial surfaces of the valves and then set the thickness of the valve to that expected surgically based on iterative testing. Further studies need to be done comparing actual valve thickness to 3DE-based measurements.

The valve leaflet coaptation zone greatly influences the presence or absence of regurgitation [27]. To date, most quantification packages and 3D printed models have not attempted to capture this region in their virtual or physical models. Our method is notably able to reproduce coaptation when it is visible in the 3D images (Figs. 1, 2, and 5). In our experience, coaptation can often be seen better from TTE images than what is typical in TEE images, presumably because the ultrasound beam is approaching the valve from the ventricular side.

Fabricating Models Suitable for Simulation

Other disciplines have demonstrated the utility of general and patient-specific surgical simulation, but to our knowledge, this is the first demonstration of 3DE-based models for surgical simulation of pediatric heart valve repair [8–11]. We first sought to print in flexible materials and then created patient-specific, 3D printed molds and fabricated silicone valves. Pediatric congenital heart surgeons and fellows simulated cutting and sewing on valve models and performed an annuloplasty and simulated CAVC repair in both valve types. Molded valves were superior for simulation as shown in Table 3.

We utilized the most flexible materials available on a high-end 3D printer and were unable to achieve optimal material properties by direct 3D printing. 3D printing is a rapidly evolving field however, and materials continue to be developed, including direct 3D printing of silicone. It is likely that with time, direct printing will be superior for rapid fabrication of patient-specific models but may require dedicated, high-cost printers. In contrast, molds offer a low-cost solution using readily available, inexpensive 3D printers as well as the option of scaling to large volume batch fabrication for groups and education (Table 2). However, it is important to emphasize that mold could be used only one time if more complicated structures such as chords and complicated anatomy were to be fabricated. Incorporation of such features may require the mold to be broken or dissolved to harvest the molded object with thin or complex parts.

Practicality

Time for segmentation varied from 30 min for a relatively normal mitral valve to over 4 h for a CAVC valve and depended greatly on the quality of the acquisition and skill at creating valve models (Table 2). While this is impractical for general usage, we are actively working on automating the virtual model creation process similar to what has been explored for adult mitral valves [26, 28]. While this will reduce time for segmentation, the time needed for printing and molding will remain, and for highly abnormal valves, automated approaches may not be applicable.

Future Directions

In the future, we hope to increase the number and types of models and demonstrate utility for simulation of difficult cases. One particularly interesting target is Ebstein abnormality of the tricuspid valve and simulation of Cone repair [29]. This is primarily a leaflet-based repair with variable leaflet sizes and a steep learning curve, and thus seems to be an attractive target for future work. Chordal models will need to be added to extend surgical simulation to the subvalvar structure, but visualization of these small structures can be difficult by all current imaging modalities. Registration of echo acquisitions from multiple views may allow optimization of ultrasound physics and resolution of orthogonal structures such as the valve leaflets in systole and the valve chordae. Extending the concept of multiple image registrations, combining leaflet models from 3DE with MRI derive models may allow printing of more complete cardiac models, leveraging the field of view of MRI and the spatial and temporal resolution of echocardiography. In the current era, valve therapies are expanding beyond open-heart surgery. There is increasing interest in catheter-based valve repairs, and the ability to practice and test new device designs on realistic valve models is appealing.

Limitations

Model creation and fabrication is currently time-intensive as is the fabrication of simulation quality valves. We utilized an expensive, high-resolution printer, and lower-resolution printers may not create models of the same fidelity. Simulation is limited to leaflet-based models and does not include the subvalvar structure. The lack of a subvalvar structure prohibits realistic liquid-based testing of atrioventricular valve function as a surgeon would do in operating room. Molding valves allows utilization of materials beyond what is offered by direct 3D printing, but do not possess fully realistic tissue properties. The modeled valves were not significantly dysfunctional, and further work will need to be done to assess the fidelity of modeling in a more diverse group, including valves with significant regurgitation or stenosis. While we compared measurements between images and fabricated models, no "gold standard" surgical or pathological measurements were available. Finally, high-quality 3D echo images can be difficult to obtain in unsedated children.

Conclusions

Patient-specific, 3DE-derived models created from 3D printed molds are a step toward realistic simulation of complex valve repairs. Molding requires more time and labor to create than directly printed models, and allows using materials that better simulate real tissue and are more economical at scale. Patient-specific simulation of valve repair in children holds promise for training and simulation of difficult cases but requires further development, particularly in the imaging and fabrication of the subvalvar structure.

Acknowledgements We would like to thank the 3D core sonographers group at The Children's Hospital of Philadelphia (CHOP) for their outstanding images as well as the 3D printing facility at CHOP and the congenital cardiac surgical fellows who tested the valves.

Funding This work was supported by the Department of Anesthesia and Critical Care at The Children's Hospital of Philadelphia, the National Institute of Biomedical Imaging and Bioengineering (NIBIB) (P41 EB015902), Cancer Care Ontario with funds provided by the Ontario Ministry of Health and Long-Term Care and the Natural Sciences and Engineering Research Council of Canada.

Compliance with Ethical Standards

Conflict of interest The authors declare they have no conflict of interest.

Ethical Approval All procedures performed on humans were in accordance with the ethical standards of the Children's Hospital of Philadelphia and with the 1964 Helsinki Declaration and its later amendments or comparable ethical standards.

References

1. Carpentier A, Chauvaud S, Mace L, Relland J, Mihaileanu S, Marino JP, Abry B, Guibourt P (1988) A new reconstructive operation for Ebstein's anomaly of the tricuspid valve. J Thorac Cardiovasc Surg 96(1):92–101
2. Chauvaud S, Perier P, Touati G, Relland J, Kara SM, Benomar M, Carpentier A (1986) Long-term results of valve repair in children with acquired mitral valve incompetence. Circulation 74(3 Pt 2):I104–I109
3. Galloway AC, Colvin SB, Baumann FG, Esposito R, Vohra R, Harty S, Freeberg R, Kronzon I, Spencer FC (1988) Long-term results of mitral valve reconstruction with Carpentier techniques in 148 patients with mitral insufficiency. Circulation 78(3 Pt 2):I97–I105
4. Mahmood F, Matyal R (2015) A quantitative approach to the intraoperative echocardiographic assessment of the mitral valve for repair. Anesth Analg 121(1):34–58. https://doi.org/10.1213/ANE.0000000000000726
5. Poelaert JI, Bouchez S (2016) Perioperative echocardiographic assessment of mitral valve regurgitation: a comprehensive review. Eur J Cardiothorac Surg 50(5):801–812. https://doi.org/10.1093/ejcts/ezw196
6. Carpentier A, Branchini B, Cour JC, Asfaou E, Villani M, Deloche A, Relland J, D'Allaines C, Blondeau P, Piwnica A, Parenzan L, Brom G (1976) Congenital malformations of the mitral valve in children: pathology and surgical treatment. J Thorac Cardiovasc Surg 72(6):854–866
7. Baird CW, Myers PO, Marx G, Del Nido PJ (2012) Mitral valve operations at a high-volume pediatric heart center: Evolving techniques and improved survival with mitral valve repair versus replacement. Ann Pediatr Cardiol 5(1):13–20. https://doi.org/10.4103/0974-2069.93704
8. Rogers-Vizena CR, Sporn SF, Daniels KM, Padwa BL, Weinstock P (2016) Cost-benefit analysis of three-dimensional craniofacial models for midfacial distraction: a pilot study. Cleft Palate Craniofac J. https://doi.org/10.1597/15-281
9. Weinstock P, Prabhu SP, Flynn K, Orbach DB, Smith E (2015) Optimizing cerebrovascular surgical and endovascular procedures in children via personalized 3D printing. J Neurosurg Pediatr. https://doi.org/10.3171/2015.3.PEDS14677
10. Helder MR, Rowse PG, Ruparel RK, Li Z, Farley DR, Joyce LD, Stulak JM (2016) Basic cardiac surgery skills on sale for $22.50: an aortic anastomosis simulation curriculum. Ann Thorac Surg 101(1):316–322. https://doi.org/10.1016/j.athoracsur.2015.08.005 (**discussion 322**)
11. Joyce DL, Dhillon TS, Caffarelli AD, Joyce DD, Tsirigotis DN, Burdon TA, Fann JI (2011) Simulation and skills training in mitral valve surgery. J Thorac Cardiovasc Surg 141(1):107–112. https://doi.org/10.1016/j.jtcvs.2010.08.059
12. Yoo SJ, Spray T, Austin EH 3rd, Yun TJ, van Arsdell GS (2017) Hands-on surgical training of congenital heart surgery using 3-dimensional print models. J Thorac Cardiovasc Surg 153(6):1530–1540. https://doi.org/10.1016/j.jtcvs.2016.12.054
13. Mahmood F, Owais K, Taylor C, Montealegre-Gallegos M, Manning W, Matyal R, Khabbaz KR (2014) Three-dimensional printing of mitral valve using echocardiographic data. JACC Cardiovasc Imaging 8(2):227–229. https://doi.org/10.1016/j.jcmg.2014.06.020
14. Muraru D, Veronesi F, Maddalozzo A, Dequal D, Frajhof L, Rabischoffsky A, Iliceto S, Badano LP (2016) 3D printing of normal and pathologic tricuspid valves from transthoracic 3D echocardiography data sets. Eur Heart J Cardiovasc Imaging. https://doi.org/10.1093/ehjci/jew215

15. Witschey WR, Pouch AM, McGarvey JR, Ikeuchi K, Contijoch F, Levack MM, Yushkevick PA, Sehgal CM, Jackson BM, Gorman RC, Gorman JH 3rd (2014) Three-dimensional ultrasound-derived physical mitral valve modeling. Ann Thorac Surg 98 (2):691–694. https://doi.org/10.1016/j.athoracsur.2014.04.094
16. Olivieri LJ, Krieger A, Loke YH, Nath DS, Kim PC, Sable CA (2015) Three-dimensional printing of intracardiac defects from three-dimensional echocardiographic images: feasibility and relative accuracy. J Am Soc Echocardiogr 28(4):392–397. https://doi.org/10.1016/j.echo.2014.12.016
17. Vukicevic M, Puperi DS, Jane Grande-Allen K, Little SH (2017) 3D printed modeling of the mitral valve for catheter-based structural interventions. Ann Biomed Eng 45(2):508–519. https://doi.org/10.1007/s10439-016-1676-5
18. Fedorov A, Beichel R, Kalpathy-Cramer J, Finet J, Fillion-Robin JC, Pujol S, Bauer C, Jennings D, Fennessy F, Sonka M, Buatti J, Aylward S, Miller JV, Pieper S, Kikinis R (2012) 3D Slicer as an image computing platform for the quantitative imaging network. Magn Reson Imaging 30(9):1323–1341. https://doi.org/10.1016/j.mri.2012.05.001
19. Knight DS, Grasso AE, Quail MA, Muthurangu V, Taylor AM, Toumpanakis C, Caplin ME, Coghlan JG, Davar J (2015) Accuracy and reproducibility of right ventricular quantification in patients with pressure and volume overload using single-beat three-dimensional echocardiography. J Am Soc Echocardiogr 28(3):363–374. https://doi.org/10.1016/j.echo.2014.10.012
20. Watanabe K, Hashimoto I, Ibuki K, Okabe M, Kaneda H, Ichida F (2015) Evaluation of right ventricular function using single-beat three-dimensional echocardiography in neonate. Pediatr Cardiol 36(5):918–924. https://doi.org/10.1007/s00246-015-1095-7
21. Schattke S, Wagner M, Hattasch R, Schroeckh S, Durmus T, Schimke I, Sanad W, Spethmann S, Scharhag J, Huppertz A, Baumann G, Borges AC, Knebel F (2012) Single beat 3D echocardiography for the assessment of right ventricular dimension and function after endurance exercise: intraindividual comparison with magnetic resonance imaging. Cardiovasc Ultrasound 10:6. https://doi.org/10.1186/1476-7120-10-6
22. Jolley MA, Ghelani SJ, Adar A, Harrild DM (2017) Three-dimensional mitral valve morphology and age-related trends in children and young adults with structurally normal hearts using transthoracic echocardiography. J Am Soc Echocardiogr 30(6):561–571. https://doi.org/10.1016/j.echo.2017.01.018
23. Pouch AM, Aly AH, Lasso A, Nguyen AV, Scanlan AB, McGowan FX, Fichtinger G, Gorman RC, Gorman JH, Yushkevich PA, Jolley MA (2017) Image segmentation and modeling of the pediatric tricuspid valve in hypoplastic left heart syndrome. Lect Notes Comput Sc 10263:95–105. https://doi.org/10.1007/978-3-319-59448-4_10
24. Kutty S, Colen T, Thompson RB, Tham E, Li L, Vijarnsorn C, Polak A, Truong DT, Danford DA, Smallhorn JF, Khoo NS (2014) Tricuspid regurgitation in hypoplastic left heart syndrome: mechanistic insights from 3-dimensional echocardiography and relationship with outcomes. Circ Cardiovasc Imaging 7(5):765–772. https://doi.org/10.1161/CIRCIMAGING.113.001161
25. Pouch AM, Xu C, Yushkevich PA, Jassar AS, Vergnat M, Gorman JH 3rd, Gorman RC, Sehgal CM, Jackson BM (2012) Semi-automated mitral valve morphometry and computational stress analysis using 3D ultrasound. J Biomech 45 (5):903–907. https://doi.org/10.1016/j.jbiomech.2011.11.033
26. Pouch AM, Wang H, Takabe M, Jackson BM, Gorman JH 3rd, Gorman RC, Yushkevich PA, Sehgal CM (2014) Fully automatic segmentation of the mitral leaflets in 3D transesophageal echocardiographic images using multi-atlas joint label fusion and deformable medial modeling. Med Image Anal 18(1):118–129. https://doi.org/10.1016/j.media.2013.10.001
27. Yamauchi T, Taniguchi K, Kuki S, Masai T, Noro H, Nishino M, Fujita S (2004) Evaluation of the mitral valve leaflet morphology after mitral valve reconstruction with a concept "coaptation length index". J Card Surg 19(6):535–538. https://doi.org/10.1111/j.0886-0440.2004.200329.x
28. Pouch AM, Aly A, Lasso A, Nguyen AV, Scanlan A, McGowan F, Fichtinger G, Gorman R, Gorman J, Yushkevich PA, Jolley M (2017) Image segmentation and modeling of the pediatric tricuspid valve in hypoplastic left heart syndrome. Lect Notes Comput Sci. https://doi.org/10.1007/978-3-319-59448-4_10
29. da Silva JP, Baumgratz JF, da Fonseca L, Franchi SM, Lopes LM, Tavares GM, Soares AM, Moreira LF, Barbero-Marcial M (2007) The cone reconstruction of the tricuspid valve in Ebstein's anomaly. The operation: early and midterm results. J Thorac Cardiovasc Surg 133(1):215–223. https://doi.org/10.1016/j.jtcvs.2006.09.018